# A Fourier Transform Infrared Absorption Difference Spectrum Associated with the Reduction of $A_1$ in Photosystem I: Are Both Phylloquinones Involved in Electron Transfer?†

Gary Hastings* and Velautham Sivakumar

*Department of Physics and Astronomy, Georgia State University, Atlanta, Georgia 30303*

*Received October 3, 2000; Revised Manuscript Received January 19, 2001*

ABSTRACT: Photoaccumulated Fourier transform infrared difference spectra associated with $P700^+$ and $P700^+A_1^-$ formation have been obtained using purified photosystem I particles from *Synechocystis* sp. PCC 6803. From these spectra, a difference spectrum associated with phylloquinone reduction ($A_1^- - A_1$) has been calculated. Infrared absorption changes associated with both the loss of the ground state and formation of the anion radical are observed in the difference spectrum. Fourier transform infrared difference spectra obtained in various spectral regions indicate that two, structurally distinct phylloquinones are photoaccumulated. This could indicate that phylloquinones on both the *PsaA* and *PsaB* branches are involved in electron transfer, and that electron transfer is bi-directional in photosystem I. It could also indicate an intrinsic structural heterogeneity in the $A_1$ binding site of the active branch. Several FTIR difference features taken together indicate that a glutamic acid residue (at position 699 or 702 on *PsaA* and/or 679 or 682 on *PsaB*) is perturbed upon $A_1$ anion formation. It is suggested that the protonation state of the perturbed glutamic acid residue is influenced by hydrogen bonding to a nearby tyrosine residue at position 696/676 on *PsaA*/*PsaB*.

In photosystem I (PS I)[1] of oxygen-evolving organisms, light absorption ultimately results in the excitation of a specialized chlorophyll (chl) donor species called P700 (*1*−*4*). The excited state is highly reducing, and an electron is transferred rapidly to a chl-like acceptor called $A_0$ (*5, 6*). The photogenerated radical pair is stabilized by a second electron transfer (ET) step from $A_0$ to a phylloquinone acceptor called $A_1$ (*1*−*4*). For purified, intact PS I particles (P700-$F_{A/B}$ particles), the phylloquinone anion is reduced by an iron−sulfur cluster, called $F_x$, in ∼200 ns at room temperature (RT) (*1*−*4*). From $F_x$ the electron is transferred to the terminal iron−sulfur centers termed $F_A$ and $F_B$.

In isolated PS I particles, at RT, the electrons on the terminal acceptors ($F_{A/B}^-$) recombine with the oxidized donor ($P700^+$) in tens of milliseconds (*1*−*4*).

By treatment of P700-$F_{A/B}$ particles with choatropic agents such as urea, the terminal acceptors, $F_A$ and $F_B$, can be selectively removed from the PS I complex (P700-$F_X$ particles) (*9*−*11*). In urea-treated PS I particles, the light-induced terminal radical pair state, $P700^+F_X^-$, recombines in ∼0.75−1.2 ms (*8, 10*). The lifetime for ET from $A_1^-$ to $F_x$ is identical to that found for the more intact system (*8*). Further treatment of PS I-$F_x$ particles with ferricyanide and urea can selectively remove $F_x$ from the PS I complex (*12, 13*). In these PS I particles, stripped of $F_A$, $F_B$, and $F_X$ (P700-$A_1$ particles), the light-induced terminal radical pair state, $P700^+A_1^-$, decays biexponentially with time constants of ∼10−15 and 150 μs, without formation of the P700 triplet state, $^3P700$ (*13, 14*).

The electron acceptor(s) $A_1$ in PS I is (are) now generally accepted to be a phylloquinone species (see refs *1*−*4* for reviews). The native PS I core contains two phylloquinone molecules, and it is unclear if one or both are involved in ET. A recent set of studies suggested a uni-directionality to the ET process (*15*). However, on the basis of sensitive pump−probe data, Joliot and Joliot (*16*) have suggested that either both phylloquinones are involved in ET, or there is an intrinsic heterogeneity in the rate of ET from $A_1^-$ to $F_x$.

A PS I crystal structure has been published at 4 Å resolution (*17*). However, the phylloquinone molecules are not well resolved, and the molecular details of phylloquinone binding in PS I are still vague (*17, 18*) (a 2.5 Å structure is expected soon where the phylloquinones are resolved).

Light-induced Fourier transform infrared (FTIR) difference spectroscopy has been utilized with much success to study quinone binding in PS II and purple bacteria (see references *19*−*22* for reviews), and much detailed structural information has been derived. Such methods rely on the photoaccumulation of a substantial static population of excited radical

† This work was supported by Georgia State University startup funds to G.H. and by Georgia State University RIG and QIF grants to G.H.

* To whom correspondence should be addressed. Email: phyggh@panther.gsu.edu. Internet: http://www.phy-astr.gsu.edu/hastings/index.html.

[1] Abbreviations: $A_0$, primary electron acceptor in photosystem I; $A_1$, secondary electron acceptor in photosystem I; (B)Chl-a, (bacterio)-chlorophyll *a*; β-DM, β-dodecyl maltoside; C=O, carbonyl; C−O, semiquinone carbonyl; DS, difference spectra or spectrum; ET, electron transfer; ESEEM, electron spin−echo envelope modulation; PS I, photosystem I; P700, primary electron donor in PS I; ps, picsecond; ns, nanosecond; μs, microsecond; ms, millisecond; PMS, phenazine methosulfate; PQ, plastoquinone; P700-$A_1$ particle, PS I particle that has been stripped of all the iron−sulfur clusters; P700-$F_X$ particle, PS I particle that has been stripped of the iron−sulfur clusters $F_A$ and $F_B$; RC, reaction center; RT, room temperature; vit-$K_1$; vitamin $K_1$ (2-methyl-3-phytyl-1,4-naphthoquinone or phylloquinone); *Rb.*, *Rhodobacter*; *Rp.*, *Rhodopseudomonas*.

10.1021/bi0023100 CCC: $20.00 
Published on Web 02/23/2001

states. The shorter the lifetime of the induced radical, the smaller the excited-state population. In intact PS I particles, the radical pair state, $P700^+F_{A/B}^-$, decays in tens of milliseconds, and the photoaccumulation of a large excited-state population is straightforward. In P700-$F_{A/B}$ and P700-$F_x$ particles, the radical pair state, $P700^+A_1^-$, decays in 200 ns and is impossible to photoaccumulate. In P700-$A_1$ particles, however, the terminal radical pair state, $P700^+A_1^-$, decays in 15−150 $\mu$s, and it is possible to photoaccumulate a small excited-state population. Extremely sensitive difference measurements are required to probe this population, however. These reasons are why the phylloquinone anion radical in PS I has never been studied in detail using FTIR difference spectroscopy.

Here we describe a series of sensitive FTIR difference measurements performed on detergent-isolated PS I particles and PS I particles that have been treated with chaotropic agents. From these experiments, we have derived IR difference spectra (DS) associated with $P700^+$ formation, and with $P700^+A_1^-$ formation. Upon comparison of these spectra, we resolve several IR difference bands that are associated with $A_1$ reduction in PS I. The most likely interpretation of the spectra is that two distinct phylloquinones are photoaccumulated.

## MATERIALS AND METHODS

Membrane fragments from the mutant psbDI/C/DII of *Synechocystis* sp. PCC 6803, which contain only the PS I reaction center (RC), were prepared as described previously (*23*). Purified PS I trimers and monomers were prepared from the membranes (*24*), and P700-$F_x$ and P700-$A_1$ particles were prepared as described (*4, 9*−*13*). The removal of $F_{A/B}$ and $F_x$ was monitored using microsecond time-resolved visible spectroscopy. In P700-$F_X$ and P700-$A_1$ particles, radical pair recombination is dominated by components with lifetimes of ∼1 ms and 10−150 $\mu$s, respectively (data not shown). This indicates the effectiveness of the sample preparation procedures.

All FTIR spectra were recorded using a Bruker IFS/66 FTIR spectrometer equipped with accessories allowing measurements from 30 000 $cm^{-1}$ (333 nm) to 700 $cm^{-1}$. PS I samples were concentrated and suspended in $D_2O$ Tris buffer, pH (not pD) ∼8.3. Approximately 20 mM ascorbate and 10 $\mu$M PMS (in $D_2O$) were added. Another approach, yielding identical results, was to incubate the sample in 1 mM ferricyanide and 1 mM ferrocyanide (in $D_2O$). The PS I samples were placed between a pair of $CaF_2$ windows, separated using Teflon spacers. All experiments described here were performed at room temperature (RT). The absorbance of the sample in the cell was ∼0.7−1.2 at the peak of the amide I absorption band (about 1653 $cm^{-1}$). Sixty-four interferograms were collected before, during, and after light excitation from a 5 mW helium−neon laser. Identical results were obtained using a white light source that had been blue (665 nm long-pass) and heat filtered (20 cm of water). The spectra collected before illumination were ratioed directly against the spectra collected during and after illumination. Thus, the absorption spectra collected represent true DS. For PS I samples incubated in ferri/ferrocyanide, several spectra were collected after excitation, since $P700^+$ has a lifetime of minutes. For PS I samples incubated in PMS/ascorbate, only a single spectrum was collected after excitation. The DS collected after light excitation were subtracted from the DS collected during excitation to cancel any residual effects of water vapor. This procedure was not necessary for a well-purged instrument. The above procedures were computer-controlled using software written in-house to run under the Bruker program OPUS 3.0. Typically, the dark−light−dark cycle was repeated 200−400 times, but thousands of cycles are possible, depending on the signal-to-noise ratio required. For all experiments described here, spectral resolution was 4 $cm^{-1}$. Data were collected between 1000 and 5000 $cm^{-1}$ unless otherwise noted. A 5000 $cm^{-1}$ long-pass filter was inserted before the sample to block actinic effects of the spectrometer helium−neon laser. The mirror velocity was 80 kHz (20 cm/s), and double-sided interferograms were collected. A Blackmann−Harris 3-term apodization function and a zero-fill factor of 2 were used. IR radiation was detected using a preamplified Graseby D313, MCT detector. Phylloquinone (vitamin $K_1$) was obtained from Sigma and used without further purification.

## RESULTS

Figure 1A shows the ($P700^+$ − P700) FTIR DS in the 5000−800 $cm^{-1}$ spectral region, obtained using trimeric P700-$A_1$ PS I particles. Data could not be obtained in the 3100−3600 $cm^{-1}$ spectral region, and the points are shown joined by a straight line. The negative/positive bands at 2112/2036 $cm^{-1}$ are due to the C≡N stretching modes of ferri/ferrocyanide, respectively. The negative/positive bands confirm that electrons are transferred to ferricyanide. Ferri/ferrocyanide vibrational modes do not contribute to absorption changes in the 1800−1200 $cm^{-1}$ spectral region. The fact that we observe identical spectra in the absence of ferri/ferrocyanide confirms this (see below). Below 1000 $cm^{-1}$, the noise level is higher but two bands close to 900 and 795 $cm^{-1}$ can still be observed (Figure 1, inset). We are currently implementing methods to study these bands in greater detail.

Figure 1B shows the same spectrum as in Figure 1A but on an expanded scale. Also shown are the corresponding spectra obtained using monomeric P700-$F_X$ and trimeric P700-$F_{A/B}$ PS I particles. The spectra obtained using intact trimeric P700-$F_{A/B}$ particles were treated with PMS and ascorbate instead of ferri/ferrocyanide. Identical spectra were also obtained using PS I membrane fragments (data not shown). All three spectra in Figure 1B display bands at virtually identical frequencies.

Figure 2A−C show the ($P700^+A_1^-$ − $P700A_1$) and ($P700^+$ − P700) FTIR DS obtained using P700-$A_1$ particles, in three spectral regions. The ($P700^+A_1^-$ − $P700A_1$) spectrum was obtained using P700-$A_1$ particles in the presence of ascorbate and PMS. The ($P700^+$ − P700) spectra in Figure 2 are taken from Figure 1A. The ($P700^+$ − P700) spectrum was scaled to the ($P700^+A_1^-$ − $P700A_1$) spectrum to produce a similar bleaching at 1697 $cm^{-1}$. The two spectra show distinct differences. These differences are a result of reduction of $A_1$. By direct subtraction of the ($P700^+$ − P700) spectrum from the ($P700^+A_1^-$ − $P700A_1$) spectrum, an IR difference spectrum (DS) associated with only $A_1$ reduction is obtained. The ($A_1^-$ − $A_1$) light-induced FTIR DS is also displayed in Figure 2A−C. When the ($P700^+A_1^-$ − $P700A_1$) DS is scaled to the 1697 $cm^{-1}$ band in the ($P700^+$ − P700)

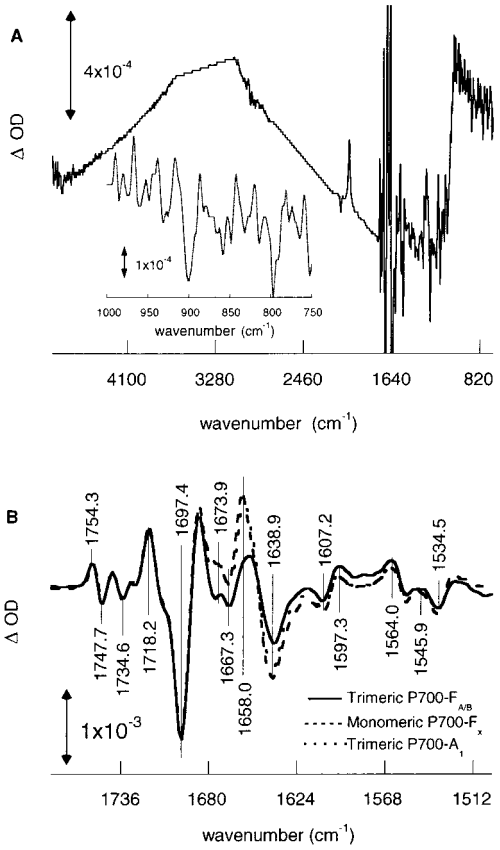


FIGURE 1: (A) ($P700^+$ − P700) FTIR DS in the 5000−700 $cm^{-1}$ spectral region, obtained using trimeric P700-$A_1$ PS I particles treated with equimolar ratios of ferri- and ferrocyanide. Inset: Expansion of the 1100−700 $cm^{-1}$ spectral region. (B) ($P700^+$ − P700) FTIR DS in the 1750−1550 $cm^{-1}$ spectral region, obtained using three types of PS I particles. The DS for the monomeric P700-$F_X$ PS I particles was obtained using equimolar ratios of ferri/ferrocyanide. The spectrum for the trimeric P700-$F_{A/B}$ PS I particles was obtained using PMS and ascorbate. The spectra have been scaled to produce similar bleachings at 1697 $cm^{-1}$. Each spectrum is obtained from a single sample and is the average of ∼12 800 interferograms.

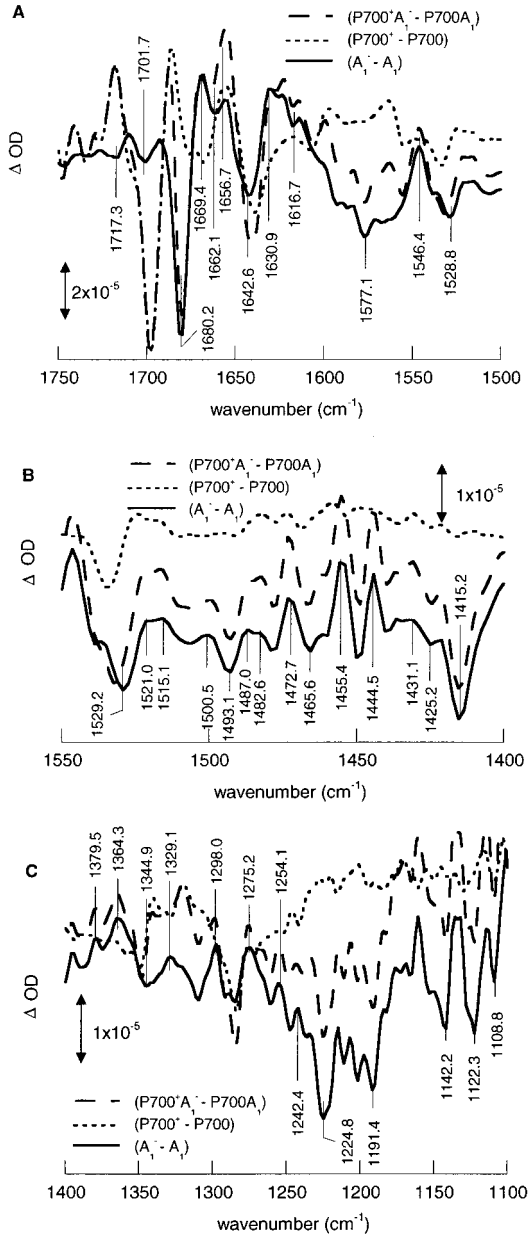


FIGURE 2: (A) FTIR DS in the 1750−1500 $cm^{-1}$ spectral region. ($P700^+$ − P700) DS from Figure 1A (•••). ($P700^+A_1^-$ − $P700A_1$) spectrum obtained using trimeric P700-$A_1$ PS I particles (− - −). ($P700^+A_1^-$ − $P700A_1$) minus ($P700^+$ − P700) double DS, labeled ($A_1^-$ − $A_1$) (—). The same three spectra are shown in the (B) 1550−1400 $cm^{-1}$ and (C) 1400−1100 $cm^{-1}$ spectral regions. The spectra were scaled to the ($P700^+A_1^-$ − $P700A_1$) spectrum to produce a similar bleaching at 1697 $cm^{-1}$. The ($P700^+A_1^-$ − $P700A_1$) spectrum is averaged over five different samples. Each spectrum, from each sample, is the average of ∼52 100 interferograms.

spectrum, direct subtraction yields a flat baseline in the 2000−5000 $cm^{-1}$ spectral region (not shown). Importantly, the ($A_1^-$ − $A_1$) spectra in Figure 2B,C are virtually unaffected by the precise scaling and subtraction procedure, since the ($P700^+$ − P700) spectrum is relatively featureless in these spectral regions.

Negative bands are related to the ground state, while positive bands are related to changes associated with the light-induced radical pair state. In the ($A_1^-$ − $A_1$) FTIR DS in Figure 2, negative bands are observed, at 1680, 1662, and 1643 $cm^{-1}$. The 1643 $cm^{-1}$ band displays a distinct shoulder near 1650 $cm^{-1}$. Between 1550 and 1400 $cm^{-1}$ (Figure 2B), positive bands are observed at 1546, 1538, 1521, 1515, 1501, 1487, 1483, 1473, 1455, and 1445 $cm^{-1}$. Negative bands are observed at 1529, 1493, 1478, 1466, 1450, and 1415 $cm^{-1}$. Below 1400 $cm^{-1}$, a strong negative band is observed at 1225 $cm^{-1}$ (Figure 2C).

Figure 3 shows the FTIR absorption spectrum of phylloquinone [vitamin $K_1$ (vit-$K_1$)] in THF, in the 1750−1250 $cm^{-1}$ spectral region. The spectrum is similar to that observed in references *25* and *26*. In the C═O and C═C stretching region, three bands are observed at ∼1662 (C═O), 1620 (C═C quinone ring), and 1597 (C═C aromatic ring) $cm^{-1}$. The 1597 $cm^{-1}$ band displays a distinct shoulder. Further bands are observed at 1462 ($CH_2$ modes), 1378 ($CH_3$ modes), and 1329, 1296 $cm^{-1}$ (C−C and C═C coupling from the double ring). Also shown in Figure 3 are the time-resolved FTIR DS obtained following UV-laser irradiation. Different spectra are observed at different times after excitation (Figure 3 inset), indicating a rather complex photochemistry for vit-$K_1$ at room temperature. This complexity is discussed in reference *26* and will be discussed in a future article.

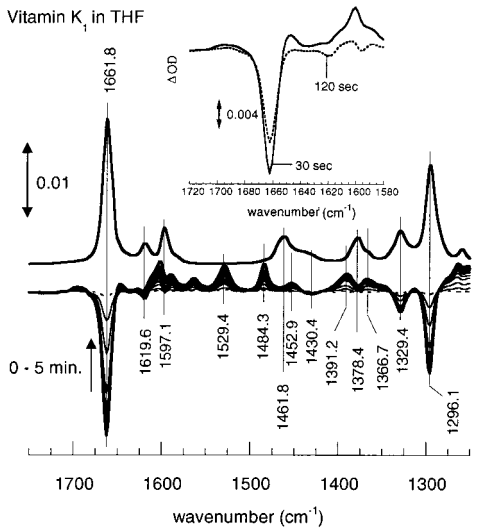


FIGURE 3: Absorbance spectrum of vitamin $K_1$ in THF (top) and time-resolved FTIR DS, obtained following a series of 20, 355 nm laser flashes at 10 Hz (bottom). The inset shows the time-resolved FTIR DS at two time delays.

## DISCUSSION

(*$P700^+$ − P700*) *FTIR DS.* The bands in FTIR DS are due to molecular group vibrations, and thus contain information with a high degree of molecular level specificity. The fact that we observe identical ($P700^+$ − P700) FTIR DS using PS I membranes (not shown), detergent-isolated monomeric or trimeric PS I particles, urea-treated P700-$F_X$ particles, and urea/ferricyanide-treated P700-$A_1$ particles indicates that (1) the detergent isolation treatment does not result in molecular level perturbations of P700 or its immediate environment, (2) the harsh conditions imposed during urea/ferricyanide treatment to strip $F_X$, $F_A$, and $F_B$ from the PS I core do not perturb P700 or its binding site, and (3) monomeric and trimeric PS I particles have identical DS.

$F_x$ is a 4Fe-4S complex which is ligated by a set of four cysteine residues (*1*−*4*). Removal of $F_x$ results in a total loss of the iron, while the labile sulfides become cross-linked to the cysteines (*4*) that held the iron atoms. $F_x$ removal should therefore affect the cysteine residues. However, these changes would be expected to show up in comparison of ($P700^+$ − P700) DS obtained using P700-$A_1$ particles and more intact particles. No such changes were observed (Figure 1) in the spectral regions considered here.

The P700-$A_1$ preparation could contain some P700-$F_x$ particles. It could also contain some particles in which the quinone binding site is damaged, with the result that only the $P700^+A_0^-$ state can form. It is doubtful, however, that these possibilities will affect the ($P700^+A_1^-$ − P700$A_1$) FTIR DS in Figure 2: First, when ET to $A_1$ is blocked, the $P700^+A_0^-$ state decays in ∼30 ns (*2*) to form the triplet state, $^3$P700, which subsequently decays in several microseconds (*1, 2, 13*). Therefore, it may be possible to photoaccumulate $^3$P700 in a portion of "damaged" reaction centers. The $^3$P700 FTIR DS is well characterized, displaying a prominent difference band at 1637(−)/1594(+) $cm^{-1}$ (*27*). No such changes are identifiable in the ($P700^+A_1^-$ − P700$A_1$) FTIR DS in Figure 2A. Therefore, this possibility is ruled out. Second, $F_x$ reduction does not lead to observable difference features in the spectral regions considered here. If active P700-$F_x$ particles do "contaminate" the P700-$A_1$ preparation, only a contribution from $P700^+$ would be expected. Since $P700^+$ contributions are subtracted from the ($P700^+A_1^-$ − P700$A_1$) FTIR DS to produce the ($A_1^-$ − $A_1$) spectrum, it is unlikely that any P700-$F_x$ particles will affect the ($A_1^-$ − $A_1$) FTIR DS.

To obtain an ($A_1^-$ − $A_1$) FTIR DS, ascorbate and PMS were used to donate electrons to $P700^+$. It is unlikely, however, that contributions from these donors contribute to the ($A_1^-$ − $A_1$) FTIR DS presented in Figure 2: PMS in $D_2O$ displays distinct absorption bands at 1627, 1606, 1554, 1398, 1370, and 1274 $cm^{-1}$ (G. Hastings, unpublished data), as was also found from electrochemically generated $PMS^-$/PMS FTIR DS (*50*). Such a pattern of negative bands is not observed in the spectra presented here. Ascorbate in $D_2O$ absorbs strongly at 1590 $cm^{-1}$, with weaker bands at 1717, 1464, 1415, and 1236 $cm^{-1}$ (G. Hastings, unpublished data). Again, such a band pattern is not observed in Figure 2. FTIR spectra for ascorbate (*51*) or the ascorbate anion (*52*) have been published but disagree with the pattern of bands found by us.

The ($P700^+$ − P700) FTIR DS has been obtained by several authors (*27*−*32*). There is agreement that the negative bands at 1748 and 1735 $cm^{-1}$ (Figure 1B) are due to the ester carbonyls (C═O's) of the chl-a molecules that constitute P700 (*27, 32*). These bands upshift to 1754 and 1741 $cm^{-1}$, respectively, upon cation formation (Figure 1B). The fact that there are two bands could indicate a dimeric nature for P700. The fact that they absorb at different frequencies indicates different environmental perturbations on each of the chl's of P700. The broad IR transition centered near 3500 $cm^{-1}$ also indicates that P700 is not a single chl species (*27, 47*). Nabedryk et al. (*28*) did not observe such an electronic transition, and suggested that the P700 cation radical was localized on a single pigment. Later the same authors did observe such an electronic transition, and accordingly suggested that the P700 cation radical is, to some degree, delocalized over two chl's.

In Figure 1B a negative band at 1697 $cm^{-1}$ is observed, in agreement with others (*27, 28*). The negative band at 1697 $cm^{-1}$ is due to the $13^1$-keto carbonyl of one (*27*) or both (*31*) of the chl-a molecules that are postulated to make up P700. Breton et al. (*27*) suggest that the 1697 $cm^{-1}$ band is due to a single chl-a keto C═O, that upshifts to 1718 $cm^{-1}$ upon cation formation, as it does in chl-a. The keto carbonyl of the other chl-a of P700 absorbs at 1639 $cm^{-1}$, and upshifts to 1658 $cm^{-1}$ upon cation formation. The origin of the positive 1687 $cm^{-1}$ band is unclear.

Hamacher et al. (*31*) studied PS I particles from *S. 6803* and found a band at 1694 $cm^{-1}$. This band is shifted by 3 $cm^{-1}$ (as are most of the other bands observed in *31*) from the corresponding band at 1697 $cm^{-1}$ observed here. Hamacher et al. indicate that the differences are due to the fact that they do not observe contributions from reduced iron−sulfur clusters. Our data would suggest that this interpretation is inappropriate because the P700 bands observed here do not shift in any of the PS I samples studied, including the PS I particles that do not contain iron−sulfur clusters. The most likely explanation is that some oxidized chl-a also contributes to the ($P700^+$ − P700) FTIR DS that was generated electrochemically (*31*).

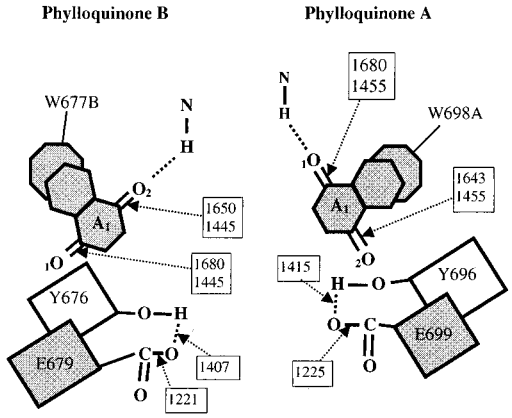


FIGURE 4: Schematic describing a possible structural model derived from the FTIR data. Phylloquinones A and B have been drawn to represent the quinones on *PsaA* and *PsaB*, but they could also represent two distinct quinones on a single branch, in which case the amino acid numbering scheme would be invalid. The band frequencies (in $cm^{-1}$) associated with particular structural elements are indicated in rectangular boxes. The amino acids are arbitrarily positioned.

The ($A_1^-$ − $A_1$) FTIR DS in Figure 2 are a result of changes due to phylloquinone anion formation. Band shifts associated with both the quinone and the binding pocket will be present. As discussed above, protein band shifts of the cysteines that could result from removal of $F_x$ from the binding pocket are not present in the spectral regions considered here.

In the following discussion, we will refer to both carbonyls of two different phylloquinones. For simplicity, we will refer to the ground-state carbonyls as $_1C{=}O_A$, $_2C{=}O_A$, $_1C{=}O_B$, and $_2C{=}O_B$. The right subscript refers to two different quinones (A or B) that do not necessarily refer to the *PsaA* or -B branch. The left subscript refers to the two carbonyls of one of the phylloquinones. We do not distinguish which carbonyl is proximal to the phytyl chain. In addition, we will refer to the semiquinone carbonyls as $_1C{-}O_A$, $_2C{-}O_A$, $_1C{-}O_B$, and $_2C{-}O_B$.

*The ($A_1^-$ − $A_1$) FTIR DS in the 1750−1500 $cm^{-1}$ Spectral Region.* In Figure 2A, the most intense negative bands are at 1680 and 1643 $cm^{-1}$. The 1643 $cm^{-1}$ band displays a slight shoulder at 1650 $cm^{-1}$. In ($Q_A^-$ − $Q_A$) FTIR studies of purple bacteria, negative bands above ∼1670 $cm^{-1}$ are generally related to protein vibrations (*19*−*21*, *25*). The intense 1680 $cm^{-1}$ band could therefore be a protein vibration(s) of residues that are tightly coupled to the phylloquinones in PS I. The intensity of the 1680 $cm^{-1}$ band is close to that of the keto C═O of P700 at 1697 $cm^{-1}$ [see the ($P700^+A_1^-$ − $P700A_1$) FTIR DS in Figure 2A]. If the intense 1680 $cm^{-1}$ band is a protein band, then it is unusually strongly perturbed upon anion formation.

Recently the phylloquinones and their binding site in PS I have been resolved at 2.5 Å. The two phylloquinones are arranged pseudosymmetrically, and have tryptophan residues $\pi$-stacked on both branches. In addition, one carbonyl of each phylloquinone is hydrogen bonded to a backbone NH (N. Krauss, personal communication; see Figure 4). The most likely residues to be strongly perturbed upon anion formation are therefore the tryptophan residues (W698/W677 on *PsaA*/*B*). However, tryptophan and its associated indole ring do not display IR absorption near 1680 $cm^{-1}$ (*43*).

A more likely explanation for the 1680 $cm^{-1}$ band is that it is associated with the carbonyl groups of $A_1$. In THF, phylloquinone C═O's display a single absorption band at 1662 $cm^{-1}$ (Figure 3). This implies a frequency upshift of 18 $cm^{-1}$ for the C═O band of $A_1$ in PS I. For hydrogen-bonded carbonyls, a downshift is expected. So the C═O groups giving rise to the 1680 $cm^{-1}$ band are probably not hydrogen bonded. Chlorophyll carbonyl frequency upshifts are common upon cation formation; for example, the ester carbonyl bands at 1748 and 1735 $cm^{-1}$ in Figure 1B are upshifted upon cation formation. Upshifting carbonyl frequencies upon semiquinone anion formation are quite unusual, but it is unclear how the C═O frequencies of $A_1$ will be affected by the $\pi$-type interaction with tryptophan. Notice that in PS II ($Q_A^-$ − $Q_A$) FTIR DS, one of the C═O modes of $Q_A$ is upshifted by 8 $cm^{-1}$ relative to the plastoquinone-9 C═O frequency observed in vitro (*53*).

Phylloquinone C═O's in vitro display a single absorption band at 1662 $cm^{-1}$ (Figure 3). In contrast, other quinones, such as ubiquinones (*25*) and plastoquinones (*53*), display two C═O bands in vitro. When ubiquinones are reconstituted into the $Q_A$ site in *Rhodobacter (Rb.) sphaeroides*, two C═O bands are still observed in the ($Q_A^-$ − $Q_A$) FTIR DS (*25*). Interestingly, when vit-$K_1$ is reconstituted into the $Q_A$ site in *Rb. sphaeroides*, two C═O bands, at 1651 and 1640 $cm^{-1}$, are now observed in ($Q_A^-$ − $Q_A$) FTIR DS (*25*), indicating a breaking of the symmetry of the C═O bonds in vit-$K_1$ upon reconstitution, which likely result from differential hydrogen bonding of both C═O's (*25*, *49*). In recent in vitro studies of plastoquinone PQ-9 (*53*), two modes were assigned to the C═O's, at 1652 and 1633 $cm^{-1}$, in good agreement with parallel normal mode calculations (*53*). For ($Q_A^-$ − $Q_A$) FTIR DS of PS II ($Q_A$ in PS II is PQ-9), the corresponding C═O bands were observed at 1659 and 1631 $cm^{-1}$. These considerations led us to assign the band observed at 1643 $cm^{-1}$ in the ($A_1^-$ − $A_1$) FTIR DS in Figure 2A to another C═O mode of $A_1$. The frequency of the mode is compatible with a hydrogen-bonded C═O mode, and it is likely that this mode corresponds to the hydrogen-bonded carbonyl observed in the 2.5 Å crystal structure.

The intensity of the 1680 $cm^{-1}$ band could result from a single quinone carbonyl (in the state $P700^+A_1^-$), or it could result from two carbonyls absorbing at the same frequency (i.e., $_1C{=}O_A$ and $_1C{=}O_B$). The latter interpretation is favored because it results in the most coherent model for all the data (see below). The intensities of the phylloquinone C═O bands at 1680 $cm^{-1}$ are near that of the keto C═O of P700. In FTIR spectroelectrochemistry studies, it has been found that the extinction coefficients of quinone C═O bands are about half that of bchl keto C═O bands in vitro (*37*). However, from comparison of ($P^+Q_A^-$ − $PQ_A$) and ($Q_A^-$ − $Q_A$) FTIR DS from purple bacteria, it is found that the donor and acceptor C═O bands have similar intensity (*20*).

If we assign the 1680 $cm^{-1}$ band to one carbonyl mode of two distinct phylloquinones in PS I ($_1C{=}O_A$, $_1C{=}O_B$), this would indicate a high degree of symmetry between the two phylloquinones, since the carbonyls absorb at identical frequency. It also indicates that two phyllosemiquinones are photoaccumulated in PS I under the conditions used here. Continuing with this interpretation, the broad band at 1643 $cm^{-1}$ and the shoulder near 1650 $cm^{-1}$ could be due to the other C═O groups of the two phylloquinones ($_2C{=}O_A$,

$_2C{=}O_B$). The band at 1650 $cm^{-1}$ is reduced in intensity due to overlap with the positive band at 1657 $cm^{-1}$.

This 1650 $cm^{-1}$ band (shoulder) is the only band discussed in this paper that is dependent on the subtraction procedure. Changing the scaling factor of the ($P700^+ - P700$) FTIR DS in Figure 2A, the 1650 $cm^{-1}$ feature can vary from a weak shoulder to a relatively intense negative band. Therefore, we believe there is a distinct negative band near 1650 $cm^{-1}$ in the ($A_1^- - A_1$) FTIR DS.

The different frequencies of $_2C{=}O_A$ (1643 $cm^{-1}$, say), $_2C{=}O_B$ (1650 $cm^{-1}$, say) indicate differing environments for each of the carbonyls. The frequencies are close to that found for either carbonyl of $Q_A$ in *Rb. sphaeroides* (*25*). In *Rb. sphaeroides* both C=O's of $Q_A$ are hydrogen bonded (*49*). This could indicate that the carbonyls $_2C{=}O_A$ and $_2C{=}O_B$ are hydrogen bonded to backbone NH groups. $_2C{=}O_A$ and $_2C{=}O_B$ absorb at different frequencies (1650 or 1643 $cm^{-1}$), so there appears to be differences in the environments of the hydrogen-bonded C=O's. This could represent a source of structural heterogeneity in the $A_1$ binding site. It could also indicate two separate phylloquinones on different branches. The origin of the positive absorption bands at 1669 and 1657 $cm^{-1}$ is unclear. One possibility is that they are related to protein backbone shifts.

The ($A_1^- - A_1$) spectra in Figure 2A are considerably more complex than electrochemically generated semiquinone FTIR DS (*37*), or UV laser-induced DS (Figure 3). This indicates that the phylloquinone binding site contributes significantly to the spectra, and/or more than a single phylloquinone, in slightly different environments, are involved in the ($A_1^- - A_1$) spectra. In *Rb. sphaeroides*, both $Q_A^-$ and $Q_B^-$ FTIR DS have been obtained. Both $Q_A$ and $Q_B$ are ubiquinones; however, the anion radical FTIR DS are very different, indicating that the quinone vibrational bands can be significantly modified by the environment.

ESEEM studies of $A_1^-$ in $^{15}N$-labeled PS I particles from *S. 6803* indicated that a tryptophan residue (W698 or W707 on *PsaA* and W677 or W686 on *PsaB*) interacts with $A_1$, possibly through a $\pi$-stacking interaction (*33*). In addition, there is weak evidence that a histidine (or asparagine or glutamine) is hydrogen bonded to one of the carbonyl oxygens of $A_1$ (*33*) [see also van der Est et al. (*34*)]. Molecular modeling studies of *S. elongatus* (*35*) indicated that the tryptophan/tyrosine pair at 698/696 on *PsaA* could be important for $A_1$ binding. Changes due to phylloquinone anion formation may therefore strongly affect these residues in PS I (see below)

*The ($A_1^- - A_1$) FTIR DS in the 1550−1400 $cm^{-1}$ Spectral Region.* In Figure 2B, the ($P700^+ - P700$) FTIR DS is relatively flat and featureless. This indicates that virtually all of the differences between the ($P700^+ - P700$) and ($P700^+A_1^- - P700A_1$) FTIR DS are due to changes associated with $A_1^-$ formation. The most intense positive bands are at 1473, 1455, and 1445 $cm^{-1}$. Two peaks are also observed at 1487 and 1483 $cm^{-1}$, and smaller bands are observed at ~1431 and 1421 $cm^{-1}$.

Quinone anions are well-known to give rise to IR absorptions in the 1500−1400 $cm^{-1}$ region (*36*−*42*, *53*). In *Rhodopseudomonas (Rp.) viridis*, a menaquinone (similar to vit-$K_1$) occupies the $Q_A$ site. ($Q_A^- - Q_A$) FTIR DS for *Rp. viridis* were found to be very similar to ($Q_A^- - Q_A$) FTIR DS obtained using *Rb. sphaeroides* RC's that had been reconstituted with vit-$K_1$ in the $Q_A$ site. Upon anion formation, three very clear bands were observed at 1478, 1444−1438, and 1392−1388 $cm^{-1}$ in ($Q_A^- - Q_A$) FTIR DS for both *Rp. viridis* and *Rb. sphaeroides* (vit-$K_1$ reconstituted) (*25*). The 1444−1438 $cm^{-1}$ mode was assigned to a predominantly C−O mode, with some C−C character. The other two bands were assigned to modes with predominantly C−C character (*25*).

It is difficult to explain the multiple bands observed in the 1550−1400 $cm^{-1}$ spectral region, based on anion absorption from a single quinone. In ($Q_A^- - Q_A$) FTIR DS from *Rps. viridis*, only three positive bands are observed upon anion formation (see above). If it is assumed that two distinct phylloquinones in PS I are involved in ET, then at least six positive bands would be required to describe the ($A_1^- - A_1$) FTIR DS in Figure 2B.

In *Rps. viridis* (and in *Rb. sphaeroides* reconstituted with vit-$K_1$) ($Q_A^- - Q_A$) FTIR DS, a single C−O band is observed, 1444−1438 $cm^{-1}$ (*25*). Similarly, a single band at 1469 $cm^{-1}$ was attributed to the semiquinone C−O stretch in PS II ($Q_A^- - Q_A$) FTIR DS (*53*). We could assign the 1455 and 1445 $cm^{-1}$ bands in Figure 2B to two C−O modes of a single quinone ($_1C{-}O_A$ and $_2C{-}O_A$). However, in *Rb. sphaeroides* RC's reconstituted with vit-$K_1$ in the $Q_A$ site, the two carbonyls of $Q_A$ are in different environments, and give rise to C=O modes at different frequencies. However, only a single, semiquinone carbonyl mode is observed (*25*). Similar conclusions were also drawn from recent ($Q_A^- - Q_A$) FTIR DS of PS II. Only a single band, at 1469 $cm^{-1}$, was attributed to the semiquinone C−O stretch. However, two modes were assigned to the C=O's at 1659 and 1631 $cm^{-1}$ (*53*). Based on these observations, we tentatively assign the 1455 and 1445 $cm^{-1}$ bands to predominantly semiquinone C−O modes of two different phylloquinones ($_1C{-}O_A$ and $_1C{-}O_B$). The slightly different frequencies of the C−O modes from different phylloquinones could indicate slightly different environments for the two semiquinone carbonyls. It could also indicate slightly different coupling strengths to phylloquinone C−C modes.

With the above assignment, and following the assignments in *Rps. viridis*, the 1487 and 1483 (or possibly the 1473) $cm^{-1}$ bands can be assigned to modes with mainly C−C character (*25*) on either phylloquinone. In addition, we can assign the 1396 and 1381 $cm^{-1}$ bands (Figure 2C) to predominantly C−C modes of two different phylloquinones (*25*). The above assignments are based upon analogy with purple bacterial systems, and we have not considered possible contributions from amino acid residues, such as glutamic acid, tyrosine, or tryptophan (see below). The main justification for this is that only quinone modes are clearly observable in the 1400−1500 $cm^{-1}$ spectral region in *Rps. viridis* ($Q_A^- - Q_A$) FTIR DS.

With these assignments, the conclusion is that two spectrally distinct phylloquinones are photoaccumulated, at least in the P700-$A_1$ particles used here. In addition, the environments of $_1C{=}O_A$ and $_2C{=}O_A$ (and $_1C{=}O_B$, $_2C{=}O_B$) are radically altered (they absorb at 1680 and 1643 $cm^{-1}$ for phylloquinone A or at 1680 and 1650 $cm^{-1}$ for phylloquinone B; see Figure 4). There is strong evidence from EPR spectroscopy (*33*−*35*) supporting the latter point. The former point could indicate that both phylloquinones in PS I are involved in ET. This is a radical conclusion but has some

merit. Recently, Joliot and Joliot (*16*) have suggested that ET in PS I involves two distinct phylloquinones. In these experiments, the authors were unable to distinguish between a model involving bi-directional ET and a model involving some heterogeneity in the $A_1$ binding site (with a single active branch). Recently, however, the kinetics of phylloquinone reoxidation have been studied in mutants where the tryptophans at 693/673 on *PsaA*/*PsaB* (*C. reinhardtii* numbering) are replaced by phenylalanines. These results have provided stronger evidence that the ET process in PS I is bi-directional, involving quinones on both branches (K. Redding, personal communication).

*Protein Contributions to the ($A_1^-$ − $A_1$) FTIR DS.* In the ($A_1^-$ − $A_1$) FTIR DS, two intense, asymmetrical, negative bands are observed at 1415 (Figure 2B) and 1225 $cm^{-1}$ (Figure 2C). Bands at these frequencies are well-known "marker bands" for protonated carboxylic acid groups (*44*). If these bands are due to COOH side-chain vibrations, then the band at 1415 $cm^{-1}$ is due to an in-plane O−H bend while the 1225 $cm^{-1}$ band is due to a C−O stretch (*44*). The small negative band at 1717 (or 1702) $cm^{-1}$ in Figure 2A could be due to the carboxylic acid C═O stretch (*44*, *45*). These considerations suggest that residues such as Glu (E) or Asp (D) are affected by $A_1^-$ formation. Conserved glutamic acid residues close to the phylloquinones are found at E699 and E702 on *PsaA*, and at E679 and E682 on *PsaB* (here we have used the numbering from *S. elongatus*; see, for example, Figure 1 in *35*). The p$K_R$ of polyglutamic acid is ∼5.1 (*41*). At physiological pH, therefore, glutamic acid is expected to be ionized. Electrostatic interactions with residue side chains could modify the p$K_R$, however. For example, a possible hydrogen bond from the conserved tyrosine residues at Y696 on *PsaA* and Y676 on *PsaB* could also contribute to partial protonation of the glutamic acid side group. The p$K_R$ of tyrosine is 10.46 (*48*). The protonation of glutamate by tyrosine is therefore energetically unfavorable, with a free energy of +60−80 kJ/mol. Electrostatic factors favor hydrogen bonding ($\Delta G \sim -10-40$ kJ/mol), however. In addition, other geometric and hydrophobicity factors could also favor hydrogen bonding. Hydrogen bonding from the OH of tyrosine to one of the oxygens of the carboxylate will lead to increased carboxylic acid character of the glutamic acid side chain. This would then provide an explanation for the bands at 1415 and 1225 $cm^{-1}$. Measurements as a function of pH are being undertaken to investigate this point. The Y696/W698 pair on *PsaA* (or Y676/W677 on *PsaB*) has been suggested to be an important combination in $A_1$ binding (*35*). Here we suggest that the Y696/W698/E699 combination on *PsaA* **and** the Y676/W677/E679 combination on *PsaB* are important for $A_1$ binding and ET. Two lines of evidence could indicate that the above Y/W/E amino acid combination is involved in phylloquinone binding on both branches. First, all three amino acids are conserved between *PsaA* and *PsaB*. Second, the 1415 and 1225 $cm^{-1}$ bands are broad, with shoulders (at 1407 and 1221 $cm^{-1}$) which could indicate two components underlying the bands. Thus, it is tempting to speculate that the photoaccumulated spectra presented here are a consequence of bi-directional ET in PS I.

The production of ($A_1^-$ − $A_1$) FTIR DS as described here relies on the use of harsh biochemical preparation procedures to produce PS I particles that have been stripped of the terminal iron−sulfur clusters. Although the molecular details underlying P700 and its binding pocket are unaffected by the treatment (see above), from transient EPR studies it was found that the spectrum of the $P700^+A_1^-$ state differed somewhat when obtained using P700-$F_{A/B}$ or P700-$F_X$ particles, compared to P700-$A_1$ particles (*54*). Based on this observation, it was suggested that removal of $F_X$ could result in changes of the protein environment around $A_1$. The fact that $A_1$ is susceptible to dark reduction by dithionite in P700-$A_1$ particles (*14*), but not in more intact particles, also indicates some modification to the $A_1$ binding site upon removal of $F_X$.

Although some alteration to the $A_1$ binding site is likely upon $F_X$ removal, no specific modifications have been suggested. Here we have identified several protein contributions to the ($A_1^-$ − $A_1$) FTIR DS. At present, it is unclear to what extent these protein contributions could result purely from the isolation procedure. For example, we cannot rule out the possibility that the protonated glutamic acid residue discussed above is a consequence of greater solvent accessibility, induced upon removal of $F_X$. The protein modes observed in the DS are the ones that are related to molecular structures that are perturbed due to the presence of an electron on phylloquinone, and hence these molecular structures are in close proximity to the phylloquinone(s). We cannot rule out the possibility that some of these protein structural components have been moved into the vicinity of the phylloquinone(s) due to modifications resulting from $F_X$ removal. Likewise, we cannot rule out the possibility that the two spectrally distinct phylloquinones observed here result from protein modifications induced upon $F_X$ removal. To test these possibilities, it is necessary to probe the $P700^+A_1^-$ radical in particles containing $F_X$. Unfortunately, it is impossible to photoaccumulate this state at room temperature in P700-$F_{A/B}$ or P700-$F_X$ PS I particles. It is possible to photoaccumulate $A_1^-$ at low temperature; however, it will still be difficult to unambiguously clarify if the observed spectral features are a result of the procedure used to produce the $A_1^-$ radical rather than an intrinsic property of the PS I particles. To circumnavigate this possible ambiguity, we are utilizing time-resolved FTIR spectroscopy to produce $P700^+A_1^-$ FTIR DS in intact PS I particles.

The complexity of the phylloquinone binding site could help explain some of the unusual properties of $A_1$. First, $A_1$ is reduced in ∼21 ps (*6*). This is an order of magnitude more rapid than the corresponding process in any other photosystem. It is not clear if the amino acids involved in the $A_1$ binding site are located between $A_0$ and $A_1$, or between $A_1$ and $F_x$. The precise locations of the amino acids could have significant influence on the observed rate of ET from $A_0$ to $A_1$.

Second, $A_1$ has an unusual redox potential. The midpoint potential of $A_1$ is ∼−800 mV, compared to −100 mV for phylloquinone in vitro (*46*). This in itself indicates strong interactions between the protein and $A_1$. Perhaps the amino acids outlined above contribute to the generation of the extreme $A_1$ redox potential. FTIR spectroscopy, in combination with site-directed mutagenesis, can be used to probe the $A_1$ binding site in PS I further. The amino acids described above represent the most likely candidates for initial site mutations.

*Summary*. It is very difficult to explain all of the IR bands in all of the spectral regions based on only two carbonyls of

one phylloquinone. The most likely explanation for all of the FTIR DS, presented here, is that two structurally distinct phylloquinones are photoaccumulated in PS I. These distinct phylloquinones could be the phylloquinones on the *PsaA* and *PsaB* branches. A partially protonated glutamic acid residue is perturbed upon $A_1$ anion formation. The protonation state is likely influenced by hydrogen bonding to a nearby tyrosine residue. It is possible that signals from two glutamic acid and tyrosine residues are observed. Both the tyrosine and glutamic acid residues are conserved on both branches, and this again could suggest that both phylloquinones in PS I are photoreduced. This in turn could indicate that ET in PS I involves both branches.

## ACKNOWLEDGMENT

We thank Charles Hopper for excellent technical assistance in the construction of accessory components for FTIR studies. Whole cells of *S. 6803* were a kind gift from Prof. Wim Vermass at Arizona State University.

## REFERENCES

1. Golbeck, G. H., and Bryant, D. A. (1991) *Curr. Top. Bioenerg. 16*, 83−175.
2. Brettel, K. (1997) *Biochim. Biophys. Acta 1318*, 322−373.
3. Golbeck, J. H. (1995) in *Advances in Photosynthesis. Molecular Biology of Cyanobacteria* (Bryant, D., Ed.) pp 311−360, Kluwer Academic Publishers, Dordrecht, The Netherlands.
4. Golbeck, J. H. (1995) in *CRC Handbook of Organic Photochemistry and Photobiology* (Bryant, D., Ed.) pp 311−360, CRC Press, Boca Raton, FL.
5. Hastings, G., Hoshina, S., Webber, A., and Blankenship, R. E. (1995) *Biochemistry 28*, 15512−15522.
6. Hastings, G., Kleinherenbrink, F. A. M., Lin, S., McHugh, T. J., and Blankenship, R. E. (1994) *Biochemistry 33*, 3193−3200.
7. Schlodder, E., Falkenberg, K., Gergeleit, M., and Brettel, K. (1998) *Biochemistry 37*, 9466−9476.
8. Luneberg, J., Fromme, P., Jekow, P., and Schlodder, E. (1994)- *FEBS Lett. 338*, 197−202.
9. Golbeck, J. H., Parrett, K. G., Mehari, T., Jones, K. L., and Brand, J. J. (1988) *FEBS Lett. 228*, 268−272.
10. Parret, K., Mehari, T., and Golbeck, J. (1990) *Biochim. Biophys. Acta 1015*, 341−352.
11. Golbeck, J., Parret, K., and McDermott, A. E. (1987) *Biochim. Biophys. Acta 893*, 149−160.
12. Warren, P. V., Golbeck, J. H., and Warden, J. T. (1993) *Biochemistry 32*, 849−857.
13. Warren, P. V., Parrett, K. G., Warden, J. T., and Golbeck, J. H. (1990) *Biochemistry 29*, 6545−6550.
14. Brettel, K., and Golbeck, J. (1995) *Photosynth. Res. 45*, 183−195.
15. Yang, F., Shen, G., Schluchter, W., Zybailov, B., Ganago, A., Vassiliev, I., Bryant, D., and Golbeck, J. (1998) *J. Phys. Chem. 102*, 8288−8299.
16. Joliot, P., and Joliot, A. (1999) *Biochemistry 38*, 11130−11136.
17. Schubert, W. D., Klukas, O., Krauss, N., Saenger, W., Fromme, P., and Witt, H. T. (1997) *J. Mol. Biol. 272*, 741−769.
18. Klukas, O., Schubert, W. D., Jordan, P., Krauss, N., Fromme, P., Witt, H., and Saenger, W. (1999) *J. Biol. Chem. 274*, 7361−7367.
19. Mäntele, W. (1993) in *The Photosynthetic Reaction Center* (Deisenhoffer, J., and Norris, J., Eds.) Vol. II, p 239, Academic Press Inc., New York.
20. Nabedryk, E. (1996) in *Infrared Spectroscopy of Biomolecules* (Mantsch, H., and Chapmann, D., Eds.) pp 39−81, Wiley-Liss, Inc., New York.
21. Mäntele, W. (1995) in *Anoxygenic Photosynthetic Bacteria* (Blankenship, R., Madigan, M., and Bauer, C., Eds.) pp 627−647, Kluwer Academic Publishers, Dordrecht, The Netherlands.
22. Breton, J., and Nabedryk, E. (1996) *Biochim. Biophys. Acta 1275*, 84−90.
23. Hastings, G., Kleinherenbrink, F., Lin, S., and Blankenship, R. (1994) *Biochemistry 33*, 3185−3192.
24. Hastings, G., Reed, J., Lin, S., and Blankenship, R. E. (1995) *Biophys. J. 69*, 2044−2055.
25. Breton, J., Burie, J., Berthomieu, C., Berger, G., and Nabedryk, E. (1994) *Biochemistry 33*, 4953−4965.
26. Burie, J. R., Boussac, A., Boullais, C., Berger, G., Mattioli, T., Mioskowski, C., Nabedryk, E., and Breton, J. (1995) *J. Phys. Chem. 99*, 4059−4070.
27. Breton, J., Nabedryk, E., and Leibl, W. (1999) *Biochemistry 38* (36), 11585−11592.
28. Nabedryk, E., Leibl, W., and Breton, J. (1996) *Photosynth. Res. 48*, 301−308.
29. Redding, K., MacMillan, F., Leibl, W., Brettel, K., Hanley, J., Rutherford, A. W., Breton, J., and Rochaix, J. D. (1998) *EMBO J. 17* (1), 50−60.
30. Nabedryk, E., Leonhard, W., Mäntele, W., and Breton, J. (1990) *Biochemistry 29*, 3242.
31. Hamacher, E., Kruip, J., Rogner, M., and Mäntele, W. (1996) *Spectrochim. Acta A 52*, 107−121.
32. Kim, S., and Barry, B. (2000) *J. Am. Chem. Soc. 122*, 4980−4981.
33. Hanley, J., Deligiannakis, Y., MacMillan, F., Bottin, H., and Rutherford, A. (1997) *Biochemistry 36*, 11543−11549.
34. van der Est, A., Prisner, T., Bittl, R., Fromme, P., Lubitz, W., Mobius, K., and Stehlik D. (1997) *J. Phys. Chem. B. 101*, 1437−1443.
35. Kamlowski, A., Altenberg-Greulich, B., van der Est, A., Zech, S., Bittl, R., Fromme, P., Lubitz, W., and Stehlik, D. (1998) *J. Phys. Chem. B 1998*, 8278−8287.
36. Juchnovski, I., and Kolev, M. (1986) *Spectrosc. Lett. 19* (10), 1183−1193.
37. Bauscher, M., Nabedryk, E., Bagley, K., Breton, J., and Mäntele, W. (1990) *FEBS Lett. 261*, 191−195.
38. Clark, B., and Evans, D. (1976) *J. Electroanal. Chem. 69*, 181−194.
39. Hienerwadel, R., Boussac, A., Breton, J., and Berthomieu, C. (1996) *Biochemistry 35*, 15447−15460.
40. Balakrishnan, G., and Umapathy, S. (1999) *J. Mol. Struct. 475*, 5−11.
41. Balakrishnan, G., Mohandas, P., and Umapathy, S. (1996) *J. Phys. Chem. 100*, 16472−16478.
42. Bauscher, M., and Mäntele, W. (1992) *J. Phys. Chem. 96*, 11101−11108.
43. Socrates, G. (1994) *Infrared Characteristic group frequencies*, 2nd ed., Wiley, New York.
44. Smith, B. (1999) in *Infrared Spectral Interpretation. A systematic approach*, p 101, CRC Press, Boca Raton, FL.
45. Venyaminov, S., and Kalnin, N. (1990) *Biopolymers 30*, 1259−127.
46. Evans, M., and Nugent, J. (1993) in *The Photosynthetic Reaction Center* (Deisenhofer, J., and Norris, J., Eds.) Vol. I, p 391, Academic Press Inc., New York.
47. Breton, J., Nabedryk, E., and Parson, W. (1992) *Biochemistry 31*, 7503−7510.
48. Voet, G., Voet, J., and Pratt, C. (1999) in *Fundamentals of Biochemistry*, p 81, Wiley, New York.
49. Lancaster, C., Ermler, U., and Michel, H. (1995) in *Anoxygenic Photosynthetic Bacteria* (Blankenship, R., Madigan, M., and Bauer, C., Eds.) pp 503−526, Kluwer Academic Publishers, Dordrecht, The Netherlands.
50. Berthomieu, C., Nabedryk, E., Breton, J., and Boussac, A. (1992) in *Research in Photosynthesis* (Murata, N., Ed.) Vol. II, pp 53−56, Kluwer Academic Publishers, Dordrecht, The Netherlands.
51. Djoman, M., Neault, J., Hasheemi-Fesharaky, S., and Tajmir-Riahi, H. (1998) *J. Biomol. Struct. Dyn. 15*, 1115−1119.

52. Neault, J., Naoui, M., and Tajmir-Riahi, H. (1995) *J. Biomol. Struct. Dyn. 13*, 387−397.
53. Razeghifard, M., Kim, S., Patzlaff, J., Hutchison, R., Krick, T., Ayala, I., Steenhuis, J., Boesch, S., Wheeler, R., and Barry, B. (1999) *J. Phys. Chem. B 103*, 9790−9800.
54. van der Est, A., Bock, C., Golbeck, J., Brettel, K., Setif, P., and Stehlik, D. (1994) *Biochemistry 33*, 11789−11797.

BI0023100